



ANALYSIS OF CRACK PROPAGATION IN AN ADHESIVE JOINT

M. D. MOHAN GIFT^{*a}, J. SELVAKUMAR^b and S. JOHN ALEXIS^c

^aDepartment of Mechanical Engineering, Panimalar Engineering College,
CHENNAI – 60210 (T.N.) INDIA

^bDepartment of Mechanical Engineering, Paavai Engineering College,
SALEM – 637108 (T.N.) INDIA

^cDepartment of Automobile Engineering, Kumaraguru College of Technology,
COIMBATORE – 641006 (T.N.) INDIA

ABSTRACT

Adhesive joints are widely used in industries because they have several advantages when compared to welded and riveted joints. One of the important factors is that they distribute the load and stresses uniformly over the entire bonded area providing good vibration resistance. Adhesive joints can readily bond dissimilar materials. The prediction of crack propagation validating the adhesive joint durability and toughness is a significant point, which is addressed through various experimental methodologies based on the type of loading conditions. The analysis is hindered by the unpredictable substrate and adhesive behavior due to the loading conditions, the nature of crack propagation, and the geometry. The impact of hardener resin ratio alteration is a parameter which needs to be explored in validating the joint toughness. The Double Cantilever Beam tests which are used for analyzing the fracture toughness for mode-I loading in adhesive joints focus on adhesive thickness variation extensively. The alteration of composition and its role in influencing the crack propagation is explored in a limited perspective. An attempt is made in this work to analyse the adhesive composition variation and its impact on the joint toughness with the help of a DCB test involving three specimens incorporating variations in the hardener resin composition. The analytical and the experimental results provided significant insights on the adhesive joint toughness validation.

Key words: Double cantilever beam, Strain energy release rate.

INTRODUCTION

Adhesive joints are known for their ability to achieve uniformity in load and stress distribution characteristics over the entire bonding region in engineering applications. They are preferred over other mechanical joints due to their fatigue resistance, crack retardation,

* Author for correspondence; E-mail: mdgift@gmail.com

galvanic isolation, vibration damping, and enhanced sealing capacity. The validation of adhesive joints is done by determination of the nature of crack propagation which requires suitable methodology. The nature of crack propagation in an adhesive joint depends widely on the loading conditions, and the hardener-resin proportion variation of the adhesive composition. The mode-1 loading conditions are more prevalent in adhesive bonding between similar and dissimilar substrates. Hence an analysis is done to estimate the nature of crack propagation under mode-1 loading conditions and variation in the hardener-resin proportion using the Double Cantilever Beam (DCB) test involving mild steel substrates and the results are presented.

Role of DCB tests

The DCB test is used to analyze the fracture behavior of adhesive joints under mode-1 loading. This test involves the measurement of the Strain Energy Release Rate (SERR or G_c) for the mode-1 loading. Some of the most prominent literatures revealing the relativity of the DCB test for the mode-1 loading is listed. Fan C. et al.¹ used the DCB test for the measurement of fracture toughness of FRP for the mode-1 loading. The experimental results were compared with the energy release rate values from the analytical methods. Andersson T. et al.² used the DCB test for measurement of the cohesive properties of an adhesive joint. Freed Y. et al.³ used a DCB specimen for prediction of the crack formation under mode-1 loading of adhesive joints involving laminated composite substrates. The fracture behavior of adhesive joints was explored by using both DCB and tapered DCB specimens by Marzi et al.⁴ Morais et al.⁵ used the DCB test to scrutinize its effectiveness when considering its application in the form of determining the fracture toughness under mode-1 loading of the cortical bone tissue. Yoshihara et al.⁶ considered the DCB test due to its effectiveness in his work involving the calculation of the strain energy release rate (G_{ic}) in the process of estimation of critical stress intensity factors of wood. C. J. Constante et al.⁷ used the DCB tests to estimate the strain energy release rate for specimens between Aluminium adherents and adhesives with varying measures of ductility.

Some of the literatures pertaining to the variations in hardener-resin proportion variation are also listed as follows. Satheesh kumar et al.⁸ investigated the influence of hardener-resin ratio changes on the behavior patterns of adhesive-bonded steel DCB specimens. The work involved the usage of both epoxy and acrylic adhesives whose hardener and resin ratios were varied. The research led to the conclusion that the transition from resin dominance to hardener dominance improved the ductility of the adhesive layer, improvement in the elongation and yield strains of the substrates. Kulkarni⁹ conducted a FEA analysis to highlight the influence of resin hardener ratio change from 1:1 to 2:1 on the sustained force for both adhesive and hybrid joints. Rupa⁹ explored the response of a

transducer to different bond strengths by considering the variations of 1:1 and 1:4 hardener-resin ratio in the selected adhesives and simultaneously maintained the consistency of the bond-line thickness.

Scope of the present research work

The research work shown in the paper explores the parameter of hardener-resin proportion variation of the adhesive bonding between steel substrates. The prominent loading conditions were selected as mode-I loading and the DCB test based on the justification from the literature was utilized for this purpose. The work aims to work on a limitation in the previous works, which did not consider the hardener-resin proportion variation as a significant parameter when conducting delaminating studies between similar as well as dissimilar substrates.

Relations used

The determination of mode I fracture toughness (G_c) is the objective of the DCB test. This involves generation of plots between the applied load and the crack length for the three composition altered specimens comprising mild steel substrates. Subsequent analysis involves plot generation between critical strain energy release rate against the crack length which in turn generates the delamination resistance curve or R curve as specified by ASTM D5528-01. The G_C calculation from the DCB test is done by considering the simple beam theory and suitable experimental compliance from equations (1) and (2).

The following equations are considered for obtaining the value for G_c .

$$G_c = \frac{1}{2B} P^2 \frac{dC}{da} \quad \dots(1)$$

$$G_c = \frac{12 P^2 a^2}{E_s B^2 h^3} \quad \dots(2)$$

$$G_i = \frac{3 P \delta}{2 B (a + |\Delta|)} \quad \dots(3)$$

The equations(1) and (2) are based on the simple beam theory and the equation(3) is based on the corrected beam theory where 'P' denotes the applied load, 'a', the crack length, 'dc/da', the degree of compliance, 'E_s', the elastic modulus of the mild steel substrates, 'b', the specimen width, and 'h', the specimen thickness.

EXPERIMENTAL

The present work analyses the results of a DCB test done on an adhesive joint having mild steel substrates and Araldite adhesive. The selection of mild steel over Aluminum as substrate material is due to the presence of a larger plastic zone in steel compared to Aluminum as outlined by Azari et al.¹⁰ The increase of adhesive plastic dissipation inside the full plastic zone was more in steel compared to aluminium as suggested by Pardoen et al.¹¹ Hence the substrates were selected as mild steel in the DCB specimen geometry which is based on ASTM D5528-01.

Table 1: Substrate properties

S. No.	Property	Value
1	Young's modulus (E)	2.1×10^5 MPa
2	Poisson's ratio (μ)	0.3
3	Density (ρ)	7850 kg/m ³

The specimens are joined using the epoxy resin Araldite LY 556 and the anhydride hardener HY 906. The adhesive is selected for its ability to perform under elevated temperatures and good fatigue resistance. Several literatures including R. Kottner et al.¹³, T. Nishioka et al.¹⁴ validate the selection of the Araldite epoxy resin.

Table 2: Araldite properties¹²

S. No.	Property	Value	Standard
1	Tensile strength	55 Mpa	ISO 527
2	Flexural modulus	3000 Mpa	ISO 178
3	Shear strength	70 Mpa	ASTM D 2344

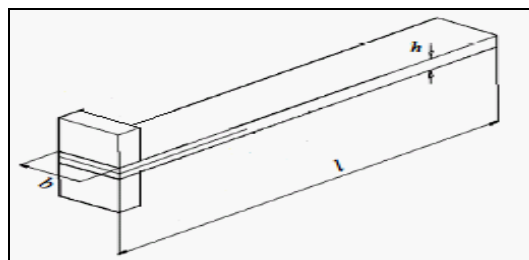


Fig. 2: ASTM standard⁹

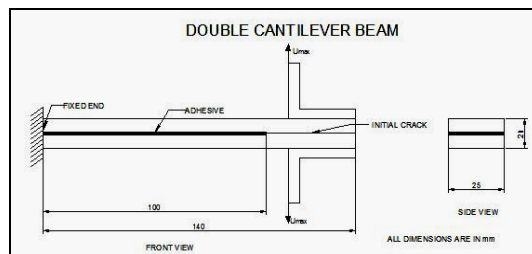


Fig. 3: DCB specimen geometry



Fig. 4: Fabricated DCB specimen

Variation of adhesive composition

The bonding surfaces of the steel substrates are scrubbed with sand paper and wiped with acetone for contamination removal. This is done to facilitate consistent load transfer and to avoid separation.

Table 3: Hardener resin variation

Specimen	% of Hardener-Resin	Hardener	Resin
A	50%-50%	5 mL	50 mL
B	60%-40%	2.5 mL	37.5 mL
C	70%-30%	2.5 mL	58.3 mL

The DCB specimens incorporating the composition alterations as specified in Table 3 were initially kept under dead weight for 8 to 10 hrs. Subsequently, they were clamped in a machine vice for an entire day and dried completely before subjecting for analysis. The adhesive thickness was maintained using a Teflon insert at 1 mm in all the three specimens. The pre-crack length was kept as 25 mm as per the ASTM standard D5528-01. A spring actuated fixture as shown in the diagram is used to clamp the DCB specimen in a tensile testing machine. The tensile testing machine comprises of a digital encoder, and a

gear rotational speed facility for systematic loading and unloading. The DCB specimens were loaded at a constant displacement rate of 1 mm/min.

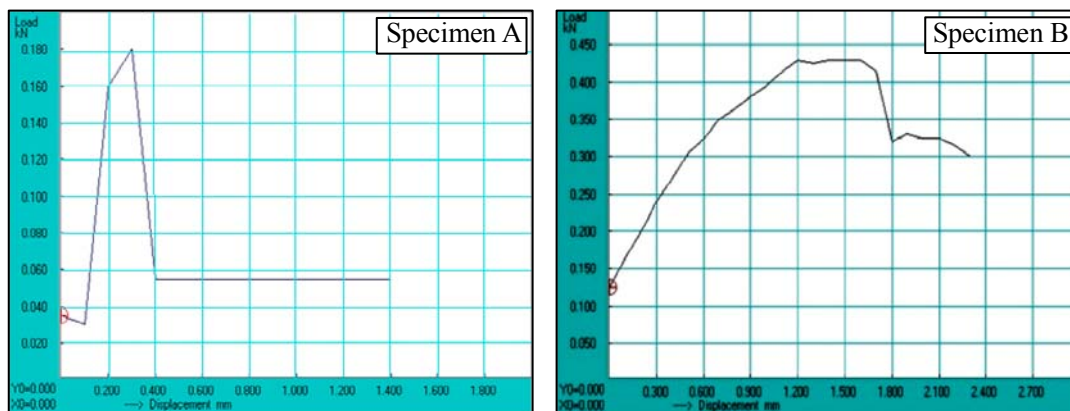


Fig. 5: Clamped DCB specimen and spring loaded fixture used in the test

RESULTS AND DISCUSSION

The load displacement curves are separately obtained from the digital read out directly from the tensile testing machine for the three DCB specimens A, B and C.

Initially, the three load displacement curves are taken separately from the UTM as shown in the Fig. 6. The three curves obtained separately from the digital read-out facility of were consolidated for the three specimens shown in Fig. 7. Furthermore, the strain energy release rate (G_{IC}) vs the crack length, which constitutes the R curves was plotted for the three specimens in Fig. 8.



Cont...

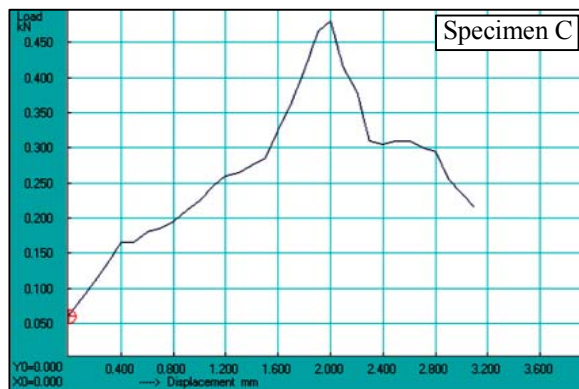


Fig. 6: P-δ curves obtained from digital read-out of the UTM separately for the 3 specimens

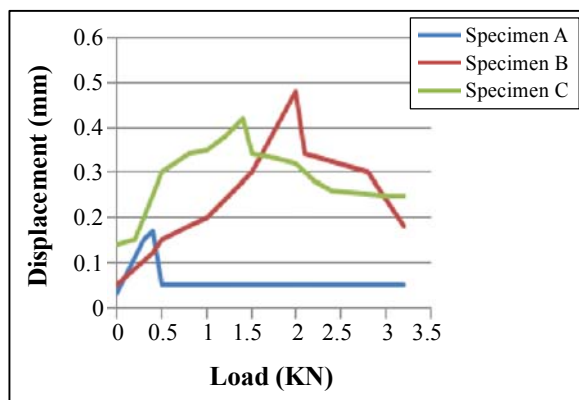


Fig. 7: Consolidated P-δ curves for the 3 specimens

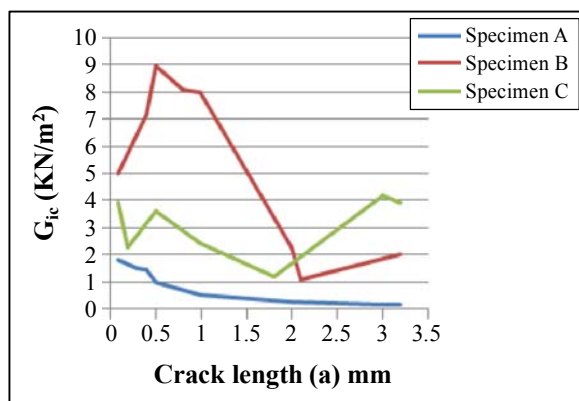


Fig. 8: Strain energy release rate (G_{Ic}) vs crack length (a) based on simple beam theory

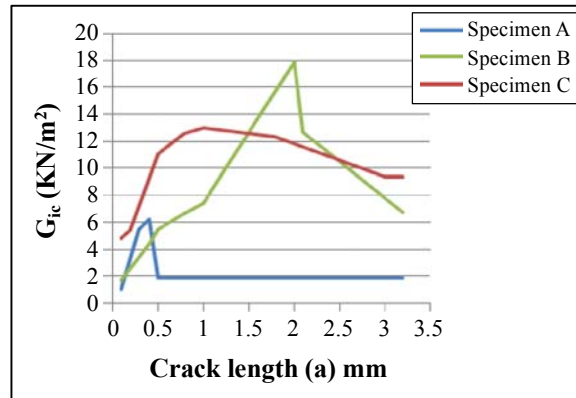


Fig. 9: Strain energy release rate (G_{ic}) vs crack length (a) based on corrected beam theory

Observations due to hardener-resin proportion variation in the adhesive layer

The observations reveal the effect of the increase in the resin composition on the load applied and the corresponding crack length in the 3 dcB specimens. In all the three types tested, the analysis involved monitoring the propagation of the crack simultaneously as the load-displacement data was plotted. The crack retardation was erratic for the first 15 mm for the first specimen which had an equal proportion of hardener-resin mixture. The remaining two specimens which had 60:40 and 70:30 showed an equal rate of propagation which lead to the finalizing of the nature of the crack as cohesive. The cracks were not found to propagate into the substrate regions for all the three specimens. Finally the conclusion of the crack propagation resulted in total detachment of the steel substrates.

Discussions and related attributes to the hardener-resin proportion variation

The $P-\delta$ curves obtained for the three specimens show convergence and marginal deviation to some extent. The Strain Energy Release Rate vs the crack length which are the R curves are drawn using the tabulations from the Simple and Corrected beam theories. The plots (Figs. 8 and 9) reveal the peak values for the G_{ic} for the specimen B which indicates the influence of the resin dominance in the adhesive composition. In all the three experimental curves in the $P-\delta$ plot, the initial linear region coincides with the obtained values. The sudden reduction in load after the peak value is attributed to an unstable crack growth during its initiation. The curve continues as linear until the starting of crack propagation which is due to the exceeding of the crack driving force over the fracture toughness of the specimens used. The R curve plotted shows a linear rise followed by a

plateau level, which indicates initial elastic behavior followed by crack length increment for all the three specimens.

Figs. 7, 8 and 9 show pronounced variations and clear differentiations of the performance of the three specimens attributed to the variation in the hardener-resin proportion. The attempt to study the propagation is quite successful incorporating the hardener-resin proportion variation with the help of the P- δ and the R curves plots.

Table 4: Range displacement tabulation

Specimen	Maximum load (KN)	Crack length (mm)	Load range (KN)	Displacement (mm)
A	0.18	0.3	0 - 0.162	0 - 0.2
			0.162 - 0.18	0.2 - 0.3
B	0.43	1.2	0 - 0.4	0 - 1.1
			0.4 - 0.43	1.1 - 1.2
C	0.48	2	0 - 0.46	0 - 1.8
			0.46 - 0.48	1.8 - 2

Table 5: G_{ic} calculation from simple beam theory

Specimen A			Specimen B			Specimen C		
a (mm)	P (KN)	G_{ic} (KN/m ²)	a (mm)	P (KN)	G_{ic} (KN/m ²)	a (mm)	P (KN)	G_{ic} (KN/m ²)
0.1	0.03	1.80	0.1	0.05	5.00	0.1	0.14	3.92
0.3	0.15	1.50	0.4	0.12	7.20	0.2	0.15	2.25
0.4	0.17	1.45	0.5	0.15	9.00	0.5	0.3	3.60
0.5	0.05	1.00	0.8	0.18	8.10	0.8	0.34	2.89
1	0.05	0.50	1	0.2	8.00	1	0.35	2.45
2	0.05	0.25	2	0.48	2.30	1.8	0.33	1.21
3	0.05	0.17	2.1	0.34	1.10	3	0.25	4.17
3.2	0.05	0.16	3.2	0.18	2.03	3.2	0.25	3.91

Table 6: G_{ic} calculation from simple beam theory

Specimen A			Specimen B			Specimen C		
a (mm)	P (KN)	G_{ic} (KN/m ²)	a (mm)	P (KN)	G_{ic} (KN/m ²)	a (mm)	P (KN)	G_{ic} (KN/m ²)
0.03	0.1	1.023	0.05	0.1	1.704	0.14	0.1	4.773
0.15	0.3	5.443	0.12	0.4	4.39	0.15	0.2	5.357
0.17	0.4	6.219	0.15	0.5	5.515	0.3	0.5	11.029
0.05	0.5	1.838	0.18	0.8	6.667	0.34	0.8	12.593
0.05	1	1.856	0.2	1	7.426	0.35	1	12.995
0.05	2	1.866	0.48	2	17.91	0.33	1.8	12.307
0.05	3	1.867	0.34	2.1	12.69	0.25	3	9.344
0.05	3.2	1.869	0.18	3.2	6.729	0.25	3.2	9.346

Research contributions derived from the work

The linkage between bonding of similar substrates and the proportion variation of the hardener and the resin was addressed in the form of effective implementation of the DCB test subjected to the mode-1 loading conditions. The scope of the other works in the realm of mode-1 testing was limited to non-consideration of the proportion variation of the adhesive selected. The present research work aims to remove this limitation by considering the three suitable variations in the proportion of the hardener-resin ratio. The two theories of G_{ic} calculations which were the Simple and Corrected beam theories provided insight as to how the influence exerted by the proportion variation impacted the bonding characteristics of the selected adhesive under mode-1 loading conditions. It is clearly visible that the linkage between the similar substrate bonding and the proportion variation impacted the G_{ic} values obtained from both the beam theories as highlighted in the plots.

CONCLUSION

An experimental attempt was made to study the nature of crack propagation in the conducted DCB test for mode-1 fracture in the adhesive joints. The DCB tests were conducted incorporating hardener resin proportion variation as an investigating parameter. The characteristics of crack propagation in the adhesive layer under the influence of hardener-resin proportion variation were analyzed. The results indicate the dominance of the

resin proportion which was visible from the R curves plotted for the three specimens incorporating the Simple and Corrected Beam theories. The analysis of the results was significant as they highlighted the retardation of the crack for the specimens B and C, which was seen from the peak Strain Energy Release Rate values from the plots.

REFERENCES

1. Chengye Fan, P. Y. Ben Jar and J. J. Roger Cheng, Cohesive Zone with Continuum Damage Properties for Simulation of Delamination Development in Fibre Composites and Failure of Adhesive Joints, *Engg. Fracture Mech.*, **75**, 3866-3880 (2008).
2. T. Anderrson and A. Biel, On the Effective Constitutive Properties of a Thin Adhesive Layer Loaded in Peel, *Int. J. Fracture*, **141(1-2)**, 227-246 (2013).
3. Yuval Freed and Leslie Banks-Sills, A New Cohesive Zone Model for Mixed Mode Interface Fracture in Biomaterials, *Engg. Fracture Mech.*, **75(15)**, 4583-4593 (2008).
4. Stephan Marzi, Anders Biel, and Ulf Stigh, On Experimental Methods to Investigate the Effect of Layer Thickness on the Fracture Behavior of Adhesively Bonded Joints, *Int. J. Adhesion and Adhesives*, **31(8)**, 840-850 (2011).
5. A. B. Morais, M. F. Moura, J. P. M. Gonçalves, P. P. Camanho, Analysis of Crack Propagation in Double Cantilever Beam Tests of Multidirectional Laminates, *Mech. Mater.*, **35(7)**, 641-652 (2010).
6. H. Yoshihara and T. Kawamura, Mode I Fracture Toughness Estimation of Wood by DCB Test, *Composites Part A: Appl. Sci. Manufacturing*, **37(11)**, 2105-2113 (2006).
7. C. J. Constante, R. D. S. G. Campilho and D. C. Moura, Tensile Fracture Characterization of Adhesive Joints by Standard and Optical Techniques, *Engg. Fracture Mech.*, **136(7)**, 292-304 (2015).
8. V. Satheesh Kumar and R. G. Narayanan, Investigation on the Influence of Adhesive Properties on the Formability of Adhesive Bonded Steel Sheets, *J. Mech. Engg. Sci.*, **228(3)**, 405-425 (2015).
9. M. Rupa, On the Characterization of Ultrasonic Response Curves for Joint Strength Correlation, *Indian J. Engg. Mater. Sci.*, **2**, 281-285 (1995).
10. S. Azari, A. Ameli, N. V. Datla, M. Papini and J. K. Spelt, Effect of Substrate Modulus on the Fatigue Behaviour of Adhesively Bonded Joints, *Mater. Sci. Engg.*, **534**, 594-602 (2012).

11. T. Pardoen, T. Ferracin, C. M. Landis and F. Delannay, Constraint Effects in Adhesive Joint Fracture, *J. Mech. Phys. Solids*, **53**, 1951-1983 (2005).
12. Huntsman Data Sheet of Araldite Adhesives for Advanced Materials, Huntsman International LLC (2001-2014).
13. R. Kottner, R. Hynek and T. Kroupa, Identification of Parameters of Cohesive Elements for Modeling of Adhesively Bonded Joints of Epoxy Composites, *Appl. Computational Mech.*, **7**, 137-144 (2013).
14. T. Nishioka and S. N. Atluri, Finite Element Simulation of Fast Fracture in Steel DCB Specimen, *Engg. Fracture Mech.*, **16(2)**, 157-175 (1982).

Accepted : 01.07.2016